

THE APPLICATION OF THE GEIGER-MÜLLER ION COUNTER  
TO THE STUDY OF THE SPACE DISTRIBUTION  
OF X-RAY PHOTOELECTRONS

BY J. A. VAN DEN AKKER AND E. C. WATSON

NORMAN BRIDGE LABORATORY OF PHYSICS, CALIFORNIA INSTITUTE OF  
TECHNOLOGY, PASADENA, CALIFORNIA

(Received May 4, 1931)

## ABSTRACT

The photographic plate in the apparatus for the magnetic analysis of x-ray photoelectrons has been replaced by a Geiger-Müller ion counter and the magnetic spectrum of the photoelectrons ejected from a thin film of gold by primary x-ray from molybdenum has been studied. Very great resolving power is obtained and considerable precision in determining the exact position of the lines (i.e. the energies of the photoelectrons). The numbers of  $L_{III}$  electrons of gold ejected by the  $K\alpha_1$  x-ray of molybdenum have been plotted as a function of the angle of ejection and compared with the theoretical longitudinal distribution predicted by Schur.

## INTRODUCTION

IN THE past many investigators<sup>1</sup> have observed the space distribution of x-ray photoelectrons in cloud expansion chambers. This method is powerful because one may observe directly the path taken by an individual photoelectron after ejection from the parent atom. In actual practice, however, the method has several shortcomings,<sup>2</sup> one of which is that except in a very few special cases the electrons coming from one level of the parent atom cannot be differentiated from those coming from another level.<sup>3</sup>

The method developed by one of the writers<sup>4</sup> enabled the longitudinal distribution of the photoelectrons to be studied as a function of both the energy of the incident photons and the level from which the electrons are ejected. While the change in relative intensities of "lines" in the "magnetic spectra" taken at various angles by this method yielded valuable information, the actual longitudinal distribution of a given group of photoelectrons could be obtained only qualitatively, because the photoelectrons were recorded photographically. With the aim of obtaining distribution curves of a more accurate nature, a new magnetic spectrograph has been constructed, in which the photographic plate has been replaced by a small Geiger-Müller tube.<sup>5</sup>

## APPARATUS

In Fig. 1 is shown the horizontal section through the centers of the slits of the new spectrograph. The photoelectrons are ejected from an exceedingly

<sup>1</sup> For a bibliography of work in this field see, e.g., Watson and Van den Akker, Proc. Roy. Soc. **A126**, 138 (1929).

<sup>2</sup> Williams, Nuttal and Barlow, Proc. Roy. Soc. **A121**, 611 (1928).

<sup>3</sup> Watson and Van den Akker, reference 1.

<sup>4</sup> Watson, Phys. Rev. **30**, 479 (1927).

<sup>5</sup> For a bibliography of work done on this extremely sensitive detector of ions see, e.g., Van den Akker, Rev. Sci. Instr. **1**, 672 (1930).

thin film of the element studied, which is deposited on a strip of celluloid 2 mm wide. This strip is supported with its length vertical, and so arranged at the axis of rotation of the apparatus that the electrons always leave the film normally to its surface. The width of the x-ray beam at the axis of rotation is about 4 mm, so that the film is included in the beam at all angular settings of the spectrograph. Each of the slits shown is  $1/64$  inch wide and  $1/4$  inch long. The slits  $S_1$  and  $S_2$  are 3 inches apart, and thus  $\rho$ , the radius of curvature of the electron orbits, is fixed at 1.5 inches. The slit  $S_3$  and the windows  $W_2$  and  $W_3$  in the Geiger-Muller tube aid in setting the angular dial shown in Fig. 2. Once this setting has been made, the Geiger-Muller tube is shifted to a new position, axis at  $O'$ , where the entrance window  $W_1$  is more directly behind  $S_2$ .

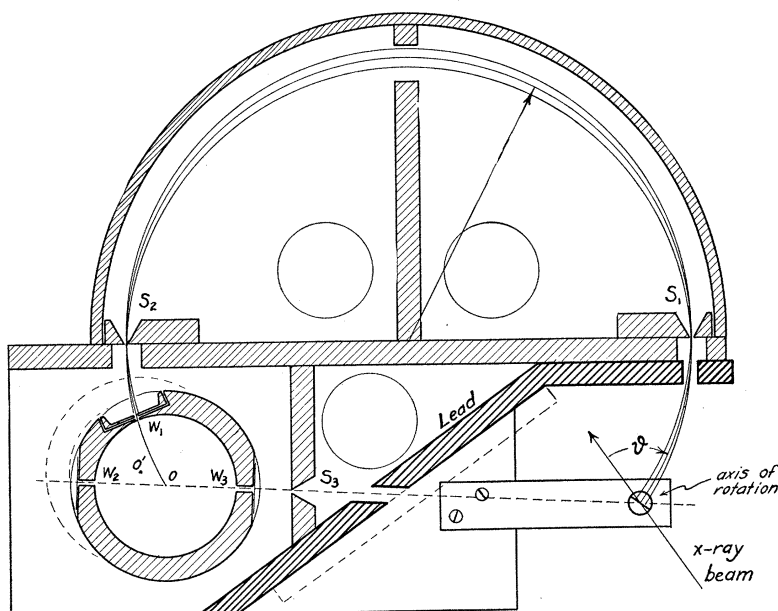


Fig. 1. Horizontal section of apparatus, showing arrangement of slits.

Rotation of the spectrograph from outside the chamber may be accomplished by means of a large brass taper, which is shown in Fig. 2. The lead-in  $B$  is a small brass pipe which connects the chamber of the Geiger-Müller tube to a gas system, while  $A$  is an electrical lead-in to the anode wire of the tube. A pointer fastened to the top of the taper enables one to read  $\theta$ , the angle between the x-ray beam and the initial direction of the photoelectrons which enter  $S_1$ .

The entrance window  $W_1$  is a set of five holes, each of 0.8 mm diameter, and arranged in a vertical line. A small disk fits into the wall of the tube, and this disk possesses five holes which fall over the five holes in the wall of the tube. This is shown in Fig. 3, in which is given a cross section of a tube of design later than that of the tube depicted in Fig. 2. A film of celluloid of the

order of  $10^{-6}$  cm thick covers the holes of the small disk. This film must satisfy two requirements: It must be sufficiently thin to pass an appreciable fraction of the slowest photoelectrons, and yet it must be sufficiently strong to withstand the difference in pressure which exists between the interior and exterior of the tube (approximately 5 cm of mercury).

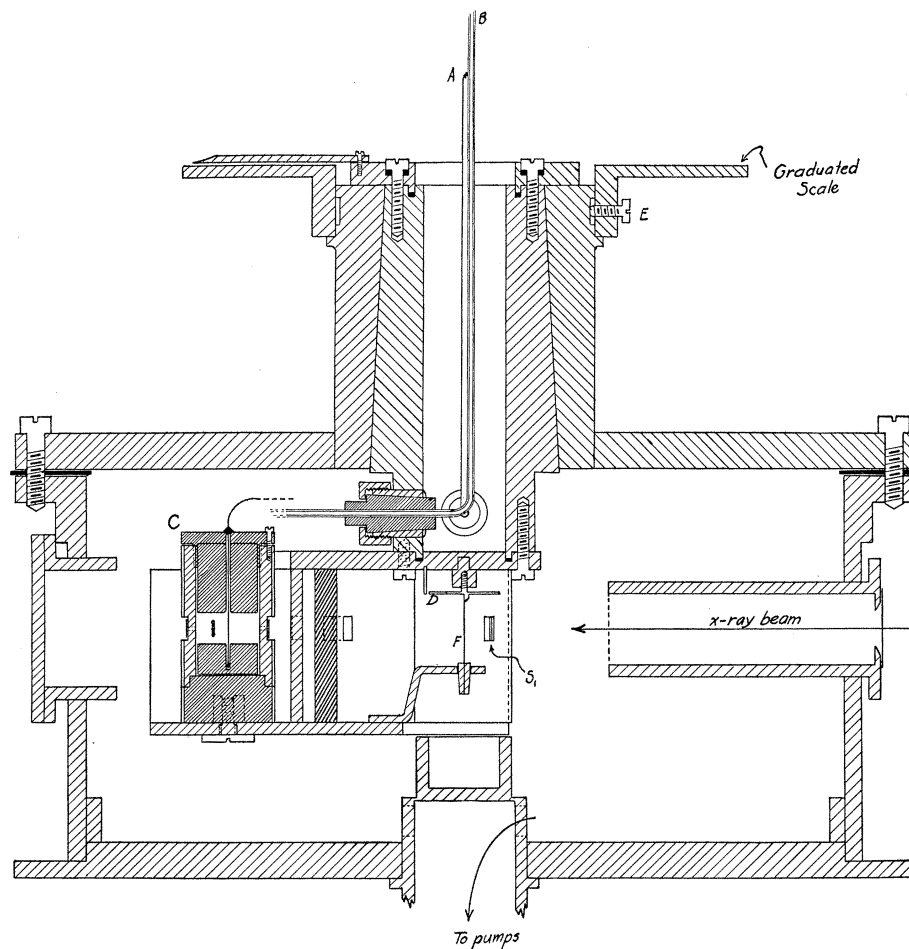


Fig. 2. Vertical section of apparatus.

A description of the specialized form of Geiger-Müller tube used in this research and of its operation has been given elsewhere.<sup>6</sup> The most important detail is the limitation of the active volume by the use of hard rubber plugs. This limitation of volume results in a very low "residual count;" and, when the anode wire is satisfactory, the electron count is independent of the potential of the anode over a range of about 50 volts. (When the whole of the

<sup>6</sup> Van den Akker, *Rev. Sci. Instr.* 1, 672 (1930).

volume of the chamber is active the effect of the ends of the tube is to make the residual count a function of the potential of the anode).

The wiring diagram for the Geiger-Müller tube is given in Fig. 4. The tube is earthed, while the anode is connected to a source of high potential through

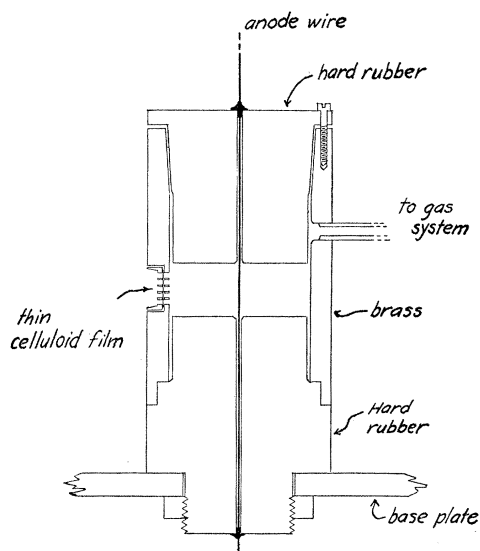


Fig. 3. Diagram of small electron counter, showing limitation of active volume by means of solid hard rubber plugs.

a resistance of  $5 \times 10^9$  ohms. Since the spectrograph is placed at the center of a long, vertical solenoid, the connector between the anode and the amplifier

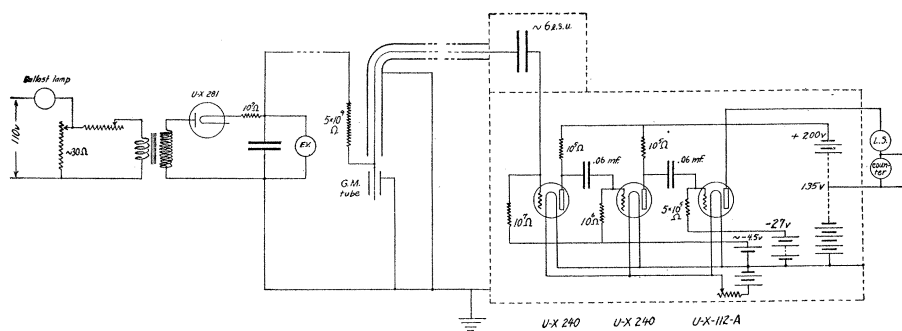


Fig. 4. General scheme of electrical connections for the Geiger-Müller tube.

is necessarily long. The strong electrical disturbances which come from the x-ray outfit make it necessary to shield this connector carefully; to satisfy this requirement, and an additional restriction on the total capacity to earth of the connector, the shielded connector is a very fine wire strung through a large lead pipe.

The results given in this paper were obtained when the x-rays were the primary rays of molybdenum, generated in a water-cooled Coolidge tube

driven at 30 kv and 20 m.a., and the electrons were ejected from a barely visible sputtered film of gold.

THE NATURE OF THE MAGNETIC SPECTRA

The results of two exploratory runs at  $\theta = 80^\circ$  are given in Figs. 5 and 6. In Fig. 5 is shown a small part of the whole spectrum which includes the double peak due to  $L_{III}$  electrons ejected from gold by  $MoK_{\alpha_{1,2}}$ . In each

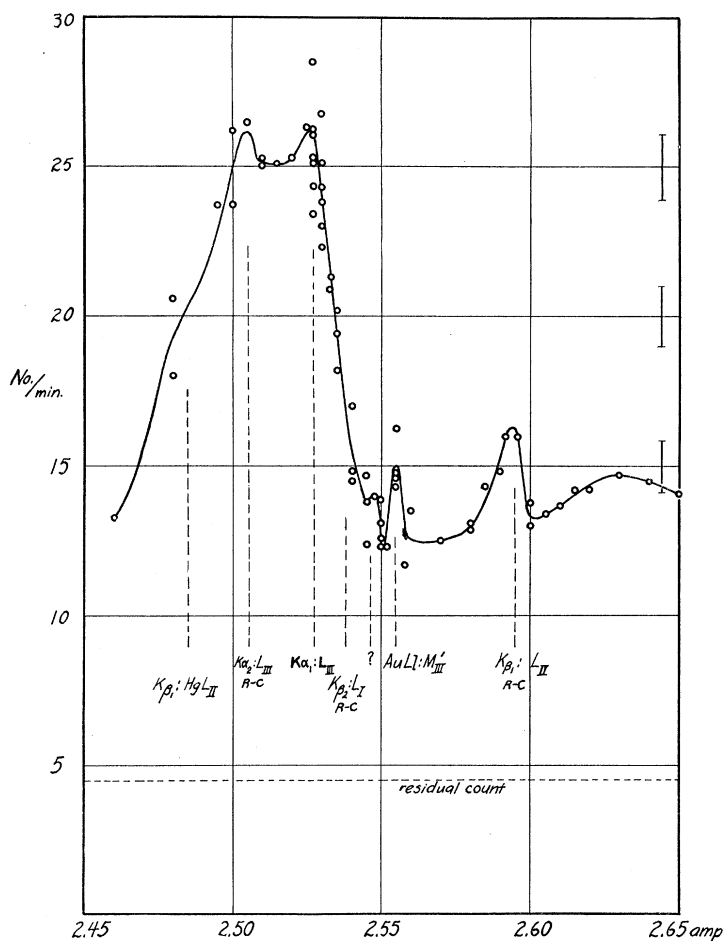


Fig. 5. A small part of the electron "spectrum" taken at  $80^\circ$ , showing the double peak due to  $L_{III}$  electrons of gold ejected by  $MoK_{\alpha_{1,2}}$ .

figure the number of impulses occurring in the Geiger-Müller tube per minute is plotted against the solenoid current. The spectrograph was calibrated with respect to the position of the  $K_{\alpha_1}: L_{III}$  peak, the  $H\rho$  value being that given by Robinson and Cassie.<sup>7</sup> All other positions indicated by vertical dashed lines were calculated. Where the precision measurements made by Robinson and

<sup>7</sup> Robinson and Cassie, Proc. Roy. Soc. A113, 282 (1928).

Cassie have been used, the letters "R-C" have been appended. In the calculation of the remaining positions, level values given in Vol. XXI of the Handbuch fur Physik were used. In all cases the  $\nu/R$  values of the emission lines of molybdenum and gold and the values of the fundamental constants were those selected by Robinson and Cassie.

The sharpness of the peaks in Fig. 5 indicates good resolution, and shows that few electrons lost appreciable energy in getting out of the sputtered film. Each point shown was obtained by a ten minute period of counting, and hence the probable error for each point was not small, being one electron per minute for points in the neighborhood of 25 per minute. The heavy vertical dashes at the extreme right of Figs. 5 and 6 represent twice the probable error of individual points. The probable error of the curves drawn is in general

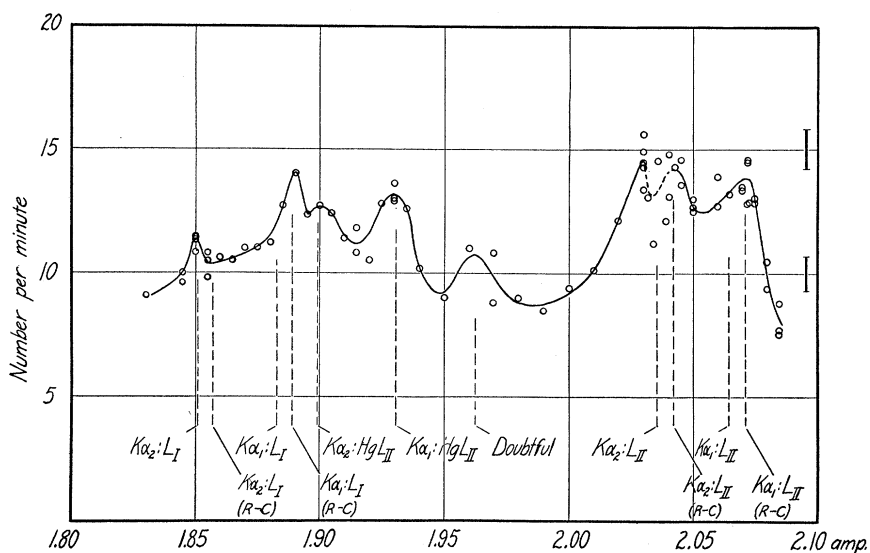


Fig. 6. The low velocity end of the electron "spectrum" showing peaks due to electrons from the  $L_I$  and  $L_{II}$  levels of gold.

somewhat smaller, being as small as 0.4 electrons per minute at certain points. The count obtained at zero magnetic field, the "residual count," was about 4.5 per minute. This count was not noticeably changed when the source of x-rays was cut off, showing that the effect of scattered x-rays was negligible.

The small peak at 2.555 amp can be attributed to electrons ejected from the  $M_{III}$  levels of gold atoms in which the transition ( $M_I \rightarrow L_{III}$ ) may occur. Thus, while the  $M_{III}$  level in the normal gold atom has the value  $\nu/R = 202.8$ , the value of this level in an atom in which the above transition may occur is 206.7. The two peaks at 1.900 and 1.930 could not be attributed to electrons coming from gold. The sputtered film of gold had been exposed to mercury vapor at room temperature, however, and hence one might reasonably expect to find peaks due to electrons from mercury. The calculated positions of electrons ejected from the mercury  $L_{II}$  level by  $MoK\alpha_{1,2}$  were, respectively, 1.931 and 1.899 amp.

THE LONGITUDINAL DISTRIBUTION OF THE  $L_{III}$  ELECTRONS

In an attempt to measure the longitudinal distribution of electrons ejected from the  $L_{III}$  level of the gold atom by  $K\alpha_1$ , the  $K\alpha_{1,2}:L_{III}$  peaks were obtained at various angles. The difference between the ordinate of the peak at 2.528 amp and the ordinate of the valley at 2.551 amp was taken as a measure of the number of electrons ejected from the  $L_{III}$  level. This difference is plotted against the angle of ejection,  $\theta$ , in Fig. 7. The deviation of the experimental curve from the points at  $60^\circ$  and  $80^\circ$  is a correction due to the loss of  $K\alpha$  rays in passing through the celluloid strip which supported the sputtered film. This correction is negligible for all angles excepting those slightly less than  $90^\circ$ . It should be noted that this correction is not accurately known, and that an error in this correction will shift the maximum of the experimental curve through several degrees.

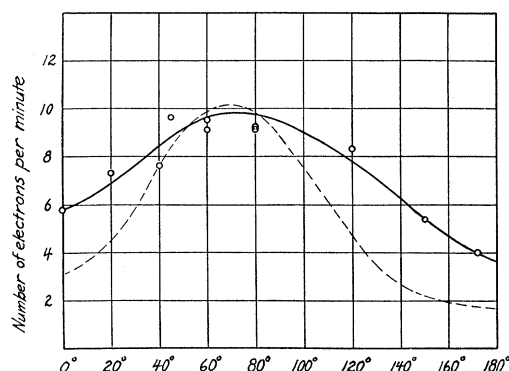


Fig. 7. The longitudinal distribution of  $L_{III}$  electrons of gold ejected by  $MoK\alpha_1$ .

Schur<sup>8</sup> has recently given a theoretical expression for the longitudinal distribution of the  $L$  electrons taken collectively. This expression is divided into two parts, one giving the distribution of the  $L_I$  electrons, and the other giving the distribution of the  $L_{II}$  and  $L_{III}$  electrons combined. The latter part is

$$J(\theta, \phi) \sim \left\{ 1 + \frac{8I_L}{h\nu} \sin^2 \theta \cos^2 \phi + \frac{2v}{c} \cos \theta \left[ 1 + 2 \left( 1 + \frac{11I_L}{h\nu} \right) \sin^2 \theta \cos^2 \phi \right] \right\}$$

where  $J(\theta, \phi)$  is the probability per unit solid angle that an electron will leave the parent atom in a direction making an angle  $\theta$  with the forward direction of the x-ray beam, and the angle  $\phi$  with the direction of the electric vector,  $\phi$  being measured in a plane perpendicular to the beam of x-rays. The quantities  $I_L$ ,  $\nu$ , and  $v$  are respectively the mean energy of binding of the  $L_{II}$  and  $L_{III}$  electrons, the frequency of the incident radiation, and the speed of ejection of the photoelectrons. Since unpolarized rays were used, we integrate with respect to  $\phi$  from 0 to  $\pi$ , and obtain

<sup>8</sup> Schur, Ann. d. Physik **4**, 433 (1930).

$$P(\theta) \sim \left\{ 1 + \frac{4I_L}{h\nu} \sin^2 \theta + \frac{2v}{c} \cos \theta \left[ 1 + \left( 1 + \frac{11I_L}{h\nu} \right) \sin^2 \theta \right] \right\}.$$

This function is represented in Fig. 7 by the dashed curve. The wide departure of the experimental curve from the theoretical at small and large angles can be explained in part by nuclear scattering of the electrons in the sputtered film. Scattering can not explain the larger part of this departure, however, as spectra obtained in the past<sup>9</sup> reveal the important fact that certain lines, strong at 80°, fall to nearly zero intensity at 0°. On the other hand, the theoretical distribution is that of the  $L_{II}$  and  $L_{III}$  electrons combined, and it may be that the distribution of the  $L_{II}$  electrons is less isotropic than that of the  $L_{III}$  electrons. The maxima of the curves are both well forward of 90°, being at about 70°, and the ratio of the ordinates at 0° and 180° of the experimental curve is nearly the same as that of the theoretical curve. The experimental value of this ratio is 1.60, while Schur's function gives

$$P(0)/P(\pi) = (1 + 2v/c)/(1 - 2v/c) = 1.82.$$

<sup>9</sup> Watson and Van den Akker, reference 1.